RECONFIGURABLE ANTENNAS AS AN ENABLING TECHNOLOGY FOR SDR

Sung-Hoon Oh (Arizona State University, Tempe, Arizona, USA; oh@asu.edu)
James T. Aberle (Arizona State University, Tempe, Arizona, USA; aberle@asu.edu)

ABSTRACT

In this paper, we establish the benefits of reconfigurable antennas at the system level, and present physical embodiments of such antennas. The reconfigurability of the antenna is achieved by electronically altering the radiating aperture based on the frequency information received by an Antenna Control Unit (ACU). The ACU consists of the Field Programmable Gate Array (FPGA) and Field Effect Transistor (FET) switches. The FPGA acts as a microcontroller to toggle FET switches to effectively change the electrical length of the antennas. As we shall show, the use of separate electronically tunable transmit and receive antennas is a promising solution for realizing multi-band SDRs.

1. INTRODUCTION

Software Defined Radios (SDRs) are considered to be the ultimate solution for the future of commercial and military wireless communications systems. However the application of SDRs over wide frequency bands is constrained at the RF front-end due to the analog hardware parts, especially the antenna [1]. By properly utilizing an intrinsically narrow band antenna whose frequency response can be dynamically controlled, the RF front-end can be simplified so that it becomes much easier to achieve the frequency agility that is needed for multi-band SDRs.

The gain-bandwidth limitation of electrically small antennas is a fundamental law of physics that limits the ability of the wireless system engineer to simultaneously reduce the size of an antenna while increasing its bandwidth and efficiency [2]. A revolutionary approach to circumventing this limitation is to construct a small, highly efficient antenna with a narrow instantaneous bandwidth that can be electronically tuned over wide frequency bands. Although this approach results in additional complexity at the antenna (since a means to control the antenna's response must be implemented), the narrow band antenna response can actually be used to reduce the need for other analog filters in the RF front-end, simplifying the overall analog

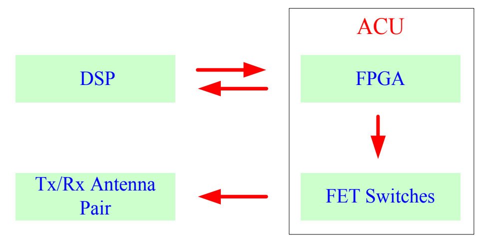

Figure 1. Block diagram of the reconfigurable antenna pair controlled by DSP.

filters in the RF front-end, simplifying the overall design problem.

The reconfigurability of the antennas is achieved by altering the geometry of the antenna electronically based on the frequency information received by an Antenna Control Unit (ACU). The ACU consists of the Field Programmable Gate Array (FPGA) and Field Effect Transistor (FET) switches. The FPGA will act as a microcontroller to toggle FET switches to effectively change the electrical length of the antennas. The block diagram of a reconfigurable antenna pair used in a SDR is shown conceptually in Figure 1. Introducing an electronically tunable antenna pair that receives commands from the radio's Digital Signal Processor (DSP) is a promising solution for realizing multi-band radios and SDRs.

The narrow instantaneous frequency response of the reconfigurable antenna pair greatly reduces the need for additional analog filtering in the RF front-end, which leads to a reduction in the size, cost, and power requirements of radios. Such an antenna pair would reject undesired interferers with a minimum degradation of the desired signal's Signal-to-Noise Ratio (SNR). In this paper, it is found that selectivity of the reconfigurable antenna pair provides filter-like performance so that duplexing, diplexing, and bandpass image rejection functions are absorbed into the antenna. In addition, a novel RF front-end architecture which is simpler and more cost-effective than current RF architectures is proposed to improve the performance of the RF front-end and demonstrate the feasibility of SDR applications.

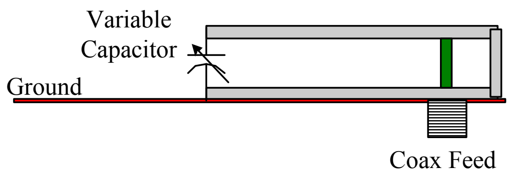

Figure 2. Geometry of SPA for reconfigurable antenna implementation.

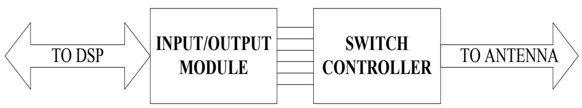

Figure 3. Block diagram outlining the functionality of the FPGA for ACU.

2. RECONFIGURABLE ANTENNA PAIR

In this section, we discuss the design of an electronically tunable Shorted Patch Antenna (SPA) controlled by an ACU consisting of FET switches and FPGA.

2.1. SHORTED PATCH ANTENNA (SPA)

SPA is one of the most promising antennas for wireless mobile devices such as mobile handsets because of their compactness, conformability, low-cost, and omni-directional patterns [3]. The SPA is loaded with small and low cost variable capacitors at the radiating edge to effectively change the electrically length of the antenna. The required physical size of SPA for resonance is also reduced by the capacitor loading.

The geometry of the SPA for the electronically tunable antenna is shown in Figure 2. The SPA is designed with a layer of copper placed above a ground plane separated by a substrate layer. The shorting edge is accomplished by connecting one side of the square radiating patch to the ground plane. To feed the SPA to the ground plane, the outer conductor of the SMA connector is connected to the ground plane while the inner conductor is connected to the patch.

It is necessary to model the antenna as a two-port device to account for the effect of its frequency response on the system. It is shown in [4] that the forward transmission coefficient (i.e., the scattering parameter, S_{21}) of the antenna is equal to its total efficiency, which includes radiation efficiency and mismatch loss. Both copper loss and tuning circuit loss contribute to reduced radiation efficiency and also affect the bandwidth. This two-port equivalent circuit of the SPA is invaluable for calculating the practical limitations on bandwidth, size, efficiency, and the effects that losses in the tuning circuits have on these quantities.

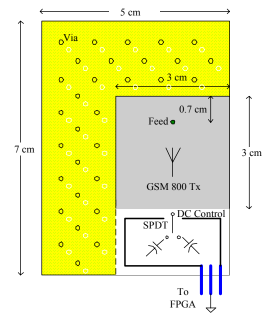

Figure 4. Dimensions of the tunable GSM 850/900 SPA mounted on a PCB with ACU.

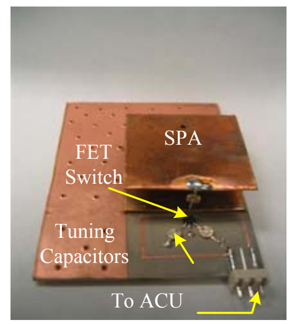

Figure 5. Photo of the fabricated tunable GSM 850/900 SPA.

2.2. ANTENNA CONTROL UNIT (ACU)

The ACU introduced in this paper employs both analog and digital technology. FET switches are adopted in order to change the electrical dimension within each antenna and to tune the antenna pair between GSM850 (US Cellular)/GSM900 and PCS/DCS bands. The On/Off status of Single Pole Double Throw (SPDT) FET switches are controlled by the FPGA based on frequency information received from the DSP. Employing the FPGA for the ACU provides the end users with complete control over the tunability of antenna.

An overall perspective view of the system level design is discussed in this section. The ACU is divided into two modules as outlined in the schematic shown in Figure 3. The input/output module receives commands from the radio's DSP and then translates them into a necessary format for the use of the switch controller. The Hardware Description Language (HDL) code residing on the input/output module of the FPGA will be responsible for the initial hand-shaking to accept data or serve as the end of the line for the transmitted data. For demonstration purposes, this module is programmed to receive frequency information in the RS-232 Asynchronous Serial Format and convert the serial data into parallel data format.

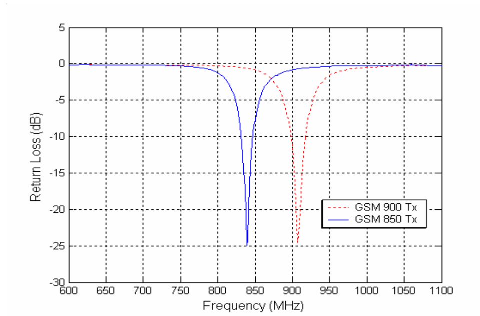

Figure 6. Measured return loss of the reconfigurable SPA between GSM 850 and GSM 900 band.

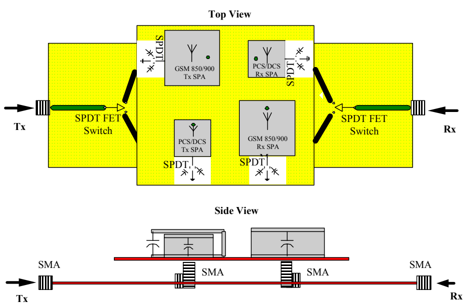

Figure 7. Prototype of tunable antennas for GSM850/900, DCS, and PCS.

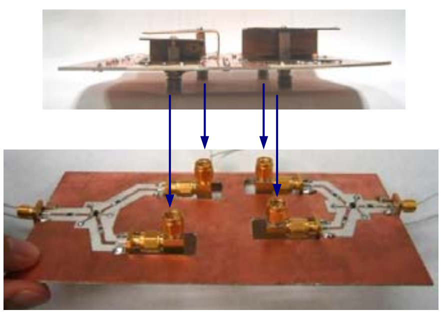

Figure 8. Photo of the prototype of tunable antennas for GSM850/900, DCS, and PCS.

The switch controller module receives parallel frequency data from the input/output module and generates required switch control signals to reconfigure the antenna pair. For SDR applications, this module can be updated anytime the RF front-end device needs to change to an application involving different frequency bands.

2.3. TUNABLE SPA DESIGN FOR GSM 850/900

An electronically tunable SPA covering the transmit portions of the US Cellular (824-849 MHz) and GSM 900 (890-915 MHz) bands was designed and fabricated in order

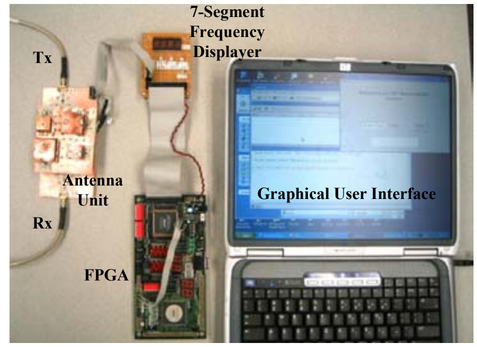

Figure 9. Test setup for demonstrating the electronically tunable antennas.

to demonstrate the feasibility of the reconfigurable antenna pair for mobile handsets. The dimensions of the antenna and the printed circuit board upon which it is mounted are shown in Figure 4. A picture of the physical hardware that was constructed is shown in Figure 5. The antenna has length, width, and height of $30 \times 30 \times 7$ *mm*, respectively. The tuning circuit consists of variable capacitors and a SPDT FET switch that is controlled by the ACU. The SPA is electronically tuned between the GSM 850 and GSM 900 bands based on the frequency information provided by the user to the FPGA. The measured return loss for both states is presented in Figure 6. The return loss of the antenna is a measure of impedance mismatch between the antenna input and its 50 Ω feeding line. The bandwidth of the antenna is, in general, determined by determining the frequency range over which the return loss is less than -10 dB. As shown in Figure 6, the bandwidth of the return loss response in each state is about equal to the 25 MHz bandwidth of the transmit portions of the US Cellular and GSM 900 bands.

2.4. TUNABLE SPA PAIR FOR GSM 850/900, DCS, AND PCS

After successfully fabricating a single SPA, two antenna pairs consisting of four individual SPAs are designed to cover all of mobile communication bands: GSM850/900, DCS, and PCS. The layout of the prototype is shown in Figure 7. The tunability between GSM and PCS/DCS bands is achieved by using two different sizes of SPAs, the larger for GSM and the smaller for PCS/DSC bands, and by switching the RF signal paths. The antenna pair for GSM bands has length, width, and height of $30 \times 30 \times 7$ *mm* and $20 \times 20 \times 6$ *mm* for PCS/DCS bands. In order to minimize the coupling and interference between each antenna pair, the antennas are arranged orthogonally relative to each other. Coupling of less than 20 dB between the Tx and Rx antennas was achieved. The tuning techniques for each SPA are described in section 2.3. The picture of the prototype is shown in Figure 8.

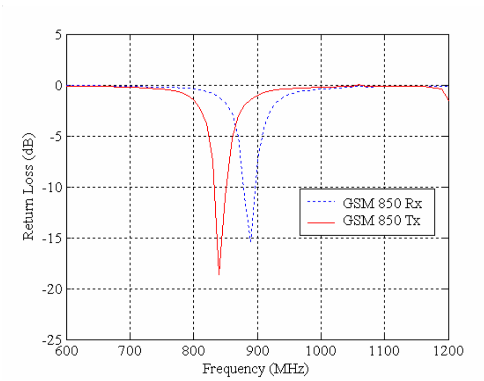

(a)

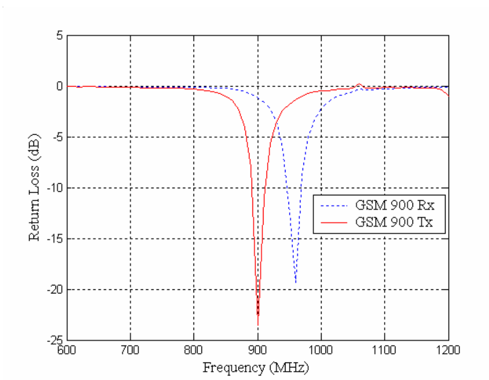

(b)

Figure 10. Measured return loss of tunable antenna pair tuned to (a) GSM 850 band and (b) GSM 900 band.

3. ELECTRONICALLY TUNABLE ANTENNA IMPLEMATATION

With the SPA pairs fully fabricated and tested as well as the ACU programmed and implemented, the setup shown in Figure 9 was assembled to evaluate the performance of the electronically tunable antenna pairs. For demonstration purposes, the DSP was emulated by a graphical user interface which accepts frequency information from a user and converts the frequency information into the required series binary format for RS-232 communication. The SPA pair is electronically tuned between GSM 850 and GSM900, and the measured return loss for each state is presented in Figure 10.

4. NOVEL RF FRONT-END FOR SDRS

Based on the careful review of antenna characteristics and experimental results revealing that the return loss of an SPA resembles the frequency response of a bandpass filter, we became interested in determining if the frequency responses of the Tx/Rx antenna pair could be used to eliminate, or reduce the requirements on the RF filters required in a wireless transceiver. Separate Tx and Rx antennas might also allow for the elimination of a T/R switch or duplex filter if enough isolation can be achieved between PA output and LNA input [5].

In order to quantify the filtering robustness of the antenna, we performed a system simulation using HP's Advanced Design System software to analyze system performance for both a conventional RF system architecture and a proposed RF system architecture based on the tunable SPA Tx/Rx pair. The specific configuration we analyzed comprises a full duplex, dual-band (GSM 850 and PCS band) superheterodyne receiver. We attempted to mimic the performance of off-the-shelf passive and active devices in our simulations. A block diagram of the conventional dual-band, full-duplex front-end is shown in Figure 11. A block diagram of a proposed novel dual-band, full-duplex front-end based on the reconfigurable antenna pair is shown in Figure 12.

The results of the simulations for the US cellular and PCS band are summarized in Table 1. It should be noted that we obtained the antenna characteristics used in the simulation from a transmission line model [6]. If we had used measured data, the results would not have been as favorable for the image rejection. As can be seen, the architecture based on the reconfigurable antenna pair offers almost the same image rejection as the conventional architecture while providing substantially better noise figure. Furthermore, the component count and cost of the SPA-pair architecture is substantial lower than that of the conventional architecture.

5. FABRICATION AND MEASUREMENTS OF RF FRONT-END ARCHITECUTRES

In order to evaluate the system level simulation results shown in Table 1, we fabricated both the conventional and the proposed RF Front-End systems using PCB technology. The block diagram and photo of the fabricated conventional dual-band, full-duplex front-end are shown in Figure 13. The block diagram and photo of the fabricated proposed dual-band front-end system are shown in Figure 14.

5.1. RECONFIGURABLE RF FRONT-END WITH ELECTRONICALY TUNABLE ANTENNA

It should be noticed that the filtering effect of the proposed RF Front-End system are achieved by the narrow band electronically tunable antenna pair. To compare the system level performance of the proposed architecture with the conventional system, the measured data of the fabricated boards are combined with antenna characteristics obtained

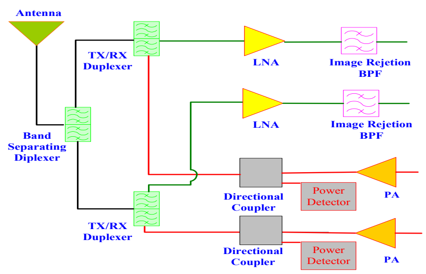

Figure 11. Conventional dual-band full-duplex RF front-end architecture.

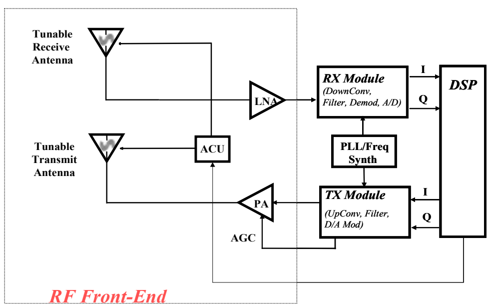

Figure 12. Proposed dual-band full duplex RF front-end implementing reconfigurable antenna pair.

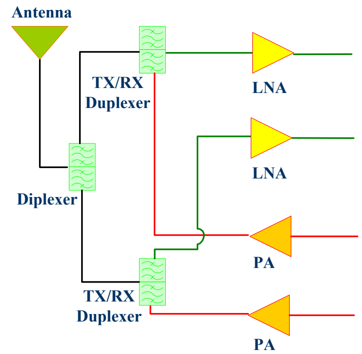

(a) Schematic

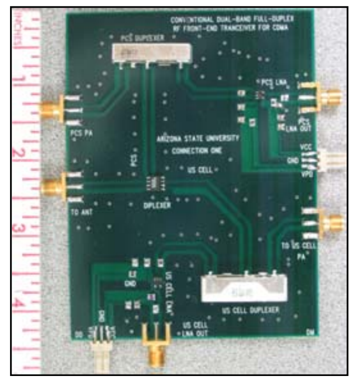

(b) Photo

Figure 13. Schematic and photo of the fabricated conventional dual-band full duplex RF front-end architecture.

from the transmission line simulation model [6]. The results are summarized in Table 2. Note that the proposed architecture with reconfigurable antenna presents almost the same image rejection as the conventional architecture.

5.2. NOISE FIGURE MEASUREMENT

The Y-factor technique was used to measure noise figures of both conventional and proposed RF Front-End receives, which involves the use of a noise source (HP Model 346B Noise Source) that has a pre-calibrated Excess Noise Ratio (ENR). The measurement results are summarized in Table 2. It is shown that the noise figure of the proposed architecture has been substantially improved by eliminating the diplexer and the duplexer used in the conventional architecture.

5.3. ANLAYSIS OF COMPONENT COUNT AND COST

Detailed analysis of component count and cost for both conventional and proposed RF front-end architecture is shown in Table 3. This result shows that the proposed RF front-end architecture is simpler and more cost-effective than current RF architectures while providing substantially better performance including the noise figure. Note that the costs shown here are the exact prices that we paid for the components and do not reflect any large quantity discounts.

6. FUTURE WORK

The reconfigurable antennas that we have breadboarded to date all use PIN diode or FET switches. These switches are far from ideal and significantly reduce the radiation efficiency of the antennas. Furthermore, these devices also exhibit non-linearities that contribute to harmonic and intermodulation distortions in both transmit and receive chains. However, RF MEMS switches appear poised to become viable alternatives in the near future to minimize these undesired effects. These switches are virtually ideal in terms of insertion loss and isolation, and their linearity is 40 to 50 dB better than GaAs devices [7, 8]. Currently, reliability and packaging issues concerning these devices are being resolved, and low cost production techniques are being developed. Based on these developments, we expect to be able to evaluate the performance of reconfigurable

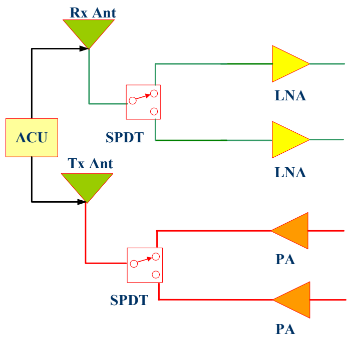

(a) Schematic

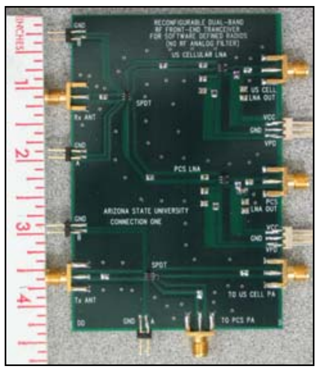

(b) Photo

Figure 14. Schematic and photo of the fabricated proposed dual-band full duplex RF front-end architecture.

antennas realized with RF MEMS switches in the near future.

In the future, we plan to automate the matching process and to expand the range of possible matching networks from four (one for each frequency band) to as many as several thousand. The hope is that after a gross match to each desired band provided by aperture reconfiguration, an automatic tuning would refine this to better than 15dB of return loss at a given operating frequency. Furthermore, extension of the antenna's ability to tune to new frequency bands could be achieved readily through a simple software upgrade, consistent with the goals of SDR.

7. CONCLUSION

A novel electronically tunable antenna pair and RF front-end architecture for current wireless communication bands (GSM 850/900, PCS, and DCS) were designed and demonstrated for SDR applications. Both high efficiency and small profile of the antenna were achieved by introducing a reconfigurable antenna pair that covers only the desired band instantaneously. Moreover, a narrowband filter-like response of the antenna pair drastically improves the SNR of RF front-end and reduces the cost and size of current radio architectures by eliminating the need for a T/R switch or a duplex filter. Since the antenna pair is electronically reconfigured based on frequency information received from the DSPs, the proposed RF-front end architecture is a promising candidate for SDRs.

8. ACKNOWLEGEMENTS

The authors would like to thank Altera Corporation for donating the FPGA board to Arizona State University. The work described in this paper was supported by Connection One, an NSF sponsored Industry University Cooperative Research Center.

9. REFERENCES

[1] B. Paul, *Software Defined Radio for 3G*. Boston: Artech House, 2003.

[2] H.A. Wheeler, "Fundamental limitations of small antennas," *Proc. IRE*, pp. 1479-1488, December 1947.

[3] C.A. Balanis, *Antenna Theory: Analysis and Design.* 2nd Ed. New York: John Wiley & Sons, INC, 1982.

[4] S.D. Rogers, J.T. Aberle, and D.T. Auckland, "Two-port model of an antenna for use in characterizing wireless communications systems obtained using efficiency measurements," *IEEE Antennas and Propagation Magazine,* vol. 45, issue 3, pp. 115–118, June 2003.

[5] D.T. Auckland, S.D. Rogers, and J.T. Aberle, "Reconfigurable antennas and RF front ends for portable wireless devices," in Proceedings of the 2002 Software Defined Radio Technical Conference, 2002, pp. 29 – 33.

[6] R. Garg, P. Bhartia, I. Bahl, and A. Ittipiboon, *Microstrip Antenna Design Handbook.* Boston: Artech House, 2003.

[7] R.B. Brown, "RF-MEMS switches for reconfigurable integrated circuits," *IEEE Transactions on Microwave Theory and Techniques*, vol. 46, pp. 1868-1880, November 1998.

[8] G.M. Rebeiz, "RF MEMS for commercial and defense applications," presented at IEEE Phoenix Chapter of MTTS, November 2003.

Architecture type	Conventional Architecture		Proposed Architecture	
Band	**GSM 850**	**PCS**	**GSM 850**	**PCS**
Desired signal at antenna	-90 dBm	-90 dBm	-90 dBm	-90 dBm
Image (200 MHz offset) at ant.	-60 dBm	-60 dBm	-60 dBm	-60 dBm
Desired signal at LNA out	-82 dBm	-80 dBm	-77 dBm	-78 dBm
Undesired signal at LNA out	-135 dBm	-120 dBm	-116 dBm	-110 dBm
Desired Signal gain	8 dB	10 dB	13 dB	12 dB
Undesired signal rejection	75 dB	60 dB	56 dB	50 dB
System noise figure	**4.1 dB**	**3.8 dB**	**1.9 dB**	**1.6 dB**

Table 1. Comparison of simulated results of conventional and proposed RF front-end Architectures.

Architecture type	Conventional Architecture		Proposed Architecture	
Band	**GSM 850**	**PCS**	**GSM 850**	**PCS**
Desired signal at antenna	-40 dBm	-40 dBm	-40 dBm	-40 dBm
Image (200 MHz offset) at ant.	-20 dBm	-20 dBm	-20 dBm	-20 dBm
Desired signal at LNA out	-26 dBm	-35 dBm	-23 dBm	-35 dBm
Undesired signal at LNA out	-41 dBm	-63 dBm	-35 dBm	-46 dBm
Desired Signal gain	14 dB	4 dB	17 dB	5 dB
Undesired signal rejection	21 dB	43 dB	15 dB	26 dB
System noise figure	**4.0 dB**	**4.8 dB**	**2.0 dB**	**4.1 dB**

Table 2. Comparison of the measured results of the conventional and the proposed RF front-end Architectures.

Architecture type	Conventional Architecture		Proposed Architecture	
	Quantity	**Unit Price USD**	**Quantity**	**Unit Price USD**
LNA	2	3.25	2	3.25
Duplexer	2	27.55	-	-
Diplexer	1	11.35	-	-
Switch	-	-	2	0.93
Total	**4**	**72.95**	**4**	**8.36**

Table 3. Comparison of component count and cost of conventional and proposed RF front-end Architectures.

